Spin-torque generation by dc or ac voltages in quasi-one-dimensional magnetic layered structures

F. Romeo[1] and R. Citro[1,2]
[1]*Dipartimento di Fisica, "E. R. Caianiello" and CNISM, Università degli Studi di Salerno, Via S. Allende, Baronissi, I-84081 Salerno, Italy*
[2]*Laboratorio Regionale SuperMat, INFM-CNR, Via S. Allende, Baronissi, I-84081 Salerno, Italy*
(Received 31 July 2009; revised manuscript received 26 November 2009; published 11 January 2010)

A general expression of the current-induced spin torque in a quasi-one-dimensional magnetic layered structure in the presence of external dc or ac voltages is derived in the framework of the scattering matrix approach. A detailed analysis is performed for a magnetic-nonmagnetic-magnetic trilayer connected to external leads in the presence of dc voltage bias in the ballistic regime. Alternatively, the possibility of producing spin torque by means of the adiabatic ac modulation of external gate voltages (quantum pumping) is proposed and discussed.

DOI: 10.1103/PhysRevB.81.045307 PACS number(s): 73.23.−b, 72.25.Pn, 75.60.Jk, 72.15.Qm

I. INTRODUCTION

Multilayers of alternating magnetic (generally ferromagnetic) and nonmagnetic metal layers have recently attracted a lot of attention because of giant magnetoresistance (GMR) and spin-valve effects. In fact their electrical resistance depends strongly on whether the moments of adjacent magnetic layers are parallel or antiparallel and this effect has allowed the development of new kinds of magnetic memory devices.[1] The origin of the GMR effect is the stronger scattering of conduction electrons by a magnetic layer when their spins lie antiparallel to the layer's magnetic moment compared to the case when their spins are parallel to the moment, while spin-valve effects originate from the spin-dependent reflection and transmission amplitudes at the interface between nonmagnetic/magnetic layers. Thus the orientations of magnetic moments can affect the flow of electrons but as a reciprocal effect a polarized electron current scattering from a magnetic layer can affect the moment of the layer itself. In fact, as proposed by Berger[2] and Slonczewski,[3] an electric current passing perpendicularly through a magnetic multilayer may exert a torque on the moments of the magnetic layers. This effect is known as *spin transfer* and may alter the magnetization state of the layer. Of course this is a different mechanism from the effects of current-induced magnetic fields and offers the possibility of realizing new kinds of magnetic devices. Importantly, it can serve as a mean to detect the spin dynamics at nanometer scale and measure spin currents. However, in order to utilize these effects in real devices, it is necessary to achieve a quantitative understanding of spin-current-induced torques and also provide different ways for their generation.

In the present literature a semiclassical Wentzel-Kramers-Brillouin approximation with spin-dependent potentials in one-dimensional (1D) systems has been proposed in Ref. 3. A generalization of this study has appeared in Ref. 4 and an extension of this calculation to take into account the band-structure effects on the degree to which an electron is transmitted through a magnetic/nonmagnetic interface has been proposed by Brataas *et al.*[5] by means of the kinetic equations for spin currents and by Waintal *et al.*[6] by using a Landauer-Büttiker-type of approach. A first-principle theory based on the spin-mixing conductance appeared in Ref. 7. The spin-transfer torque has also been analyzed in magnetic tunnel junctions by first-principles electronic-structure calculations[8] or by Boltzmann equation[9] and recently it has been revisited in the Stoner model by scattering theory[10] and in spin valves by first principles with the aid of scattering wave function.[11] *Ab initio* studies of the spin torque in GMR junctions are reported in Ref. 12.

Here we present a general formalism based on the scattering matrix approach to calculate the torques in a quasi-one-dimensional magnetic layered structure in the ballistic regime. Then we use this formalism to make an explicit calculation for a magnetic (M)-nonmagnetic (NM)-magnetic (M) trilayer connected to two metallic external leads. In this case the ballistic regime is characterized by a spin-diffusion length l_s and a mean-free path l_m larger than the NM spacer. We perform first the calculation in the presence of a dc voltage bias applied to the leads, or equivalently for currents perpendicular to the microstructure, then we propose an alternative way of achieving a spin torque by the adiabatic ac modulation of two system parameters (in our case the barrier heights at the M-NM interface), i.e., by a quantum pump mechanism.[13] The organization of the paper is the following: in Sec. II we introduce the model Hamiltonian and the general expression for the spin torque and the torkance. In Sec. III we develop the scattering matrix approach generalized for the calculation of the spin torque in a magnetic layered structure. In Sec. IV we discuss the adiabatic quantum pumping of spin torque, while in Sec. V we present the results for a specific system, a trilayer of M-NM-M metals connected to two nonmagnetic leads. A quantitative analysis of the torkance is presented both in the case of a dc bias applied to the external leads and when a quantum pump mechanism is activated. Section VI is devoted to the analysis of the spin torque generated in the spin-valve case on the free layer under dc or ac forcing terms. The two ways of generating a spin torque present some differences that are comparatively discussed. These differences could be important for the realization of new magnetic devices.

II. MODEL AND FORMALISM

Let us consider a 1D system whose Hamiltonian is: $H=-\frac{\hbar^2}{2m}\partial_x^2+V(x,\vec{\sigma})$, where $V(x,\vec{\sigma})$ is some spin-dependent

potential operator. The field operator describing the electron state Ψ, obeys the Schrödinger equation $\vec{H}\Psi = i\hbar\partial_t\Psi$ and $\Psi^\dagger\overleftarrow{H} = -i\hbar\partial_t\Psi^\dagger$ and the time evolution of the electron charge density $\rho = \Psi^\dagger e\Psi$ is determined by the Heisenberg equation:

$$\partial_t(\Psi^\dagger e\Psi) = \frac{ie}{\hbar}[\Psi^\dagger(\overleftarrow{H} - \vec{H})\Psi] = -\partial_x J, \tag{1}$$

where $J = \Psi^\dagger e\hat{v}\Psi$ is the current density while $\hat{v} = \frac{i\hbar}{2m}(\overleftarrow{\partial}_x - \vec{\partial}_x)$ is the velocity operator along the x direction. From Eq. (1) the well-known continuity equation $\partial_t\rho + \partial_x J = 0$ is obtained.

In an analogous manner, the time evolution of the spin density $S_\mu = \Psi^\dagger\frac{\hbar}{2}\sigma_\mu\Psi$, $\mu = \{x, y, z\}$ (σ_μ are the Pauli matrices), can be derived

$$\partial_t S_\mu = -\partial_x J^s_\mu + \tau_\mu. \tag{2}$$

Here $J^s_\mu = \Psi^\dagger\frac{\hbar}{2}\sigma_\mu\hat{v}\Psi$ is the μth component of the spin-current density[14] and τ_μ is the density of spin torque. When the spin-dependent potential describes the Zeeman interaction between the spin and a magnetic field along the direction $\hat{n}(x)$, $V(x, \vec{\sigma}) = \gamma(x)\hat{n}(x)\cdot\vec{\sigma}$, the density of spin torque is explicitly given by

$$\tau_\mu = \gamma(x)\Psi^\dagger[\hat{n}(x)\times\vec{\sigma}]_\mu\Psi = \frac{2\gamma(x)}{\hbar}[\hat{n}(x)\times\vec{S}]_\mu.$$

When $\gamma(x) = 0$, the spin-torque term vanishes and a continuity equation is obeyed by the spin currents, $\partial_t\vec{S} + \partial_x\vec{J}^s = 0$. In the case of a system in which a magnetic central region $x \in [-a, a]$ is connected to two external nonmagnetic leads, under the stationary condition for the spin current (i.e., $\partial_t\vec{S} = 0$) the spin torque per unit of area can be calculated by spatial integration of the equation $\partial_x J^s_\mu = \tau_\mu$ along the x direction

$$\vec{J}^s_R - \vec{J}^s_L = \int_{-a}^{+a} dx\vec{\tau} = \vec{\mathcal{T}}, \tag{3}$$

where $\vec{J}^s_{R/L} = \vec{J}^s(\pm\infty)$ is the value of the current at infinity. The above result tells that the spin torque per unit of area is due to the difference of the spin currents on the right and on the left of the magnetic scattering region. In the following section we analyze the spin-torque transfer within a scattering matrix approach.

III. DENSITY OF SPIN CURRENT WITHIN THE SCATTERING APPROACH

In order to calculate the spin torque through a magnetic region we employ the scattering matrix formalism of Ref. 15 and consider a single-channel approximation to simplify the derivation. The S matrix connects the outgoing states to the incoming states through the relation

$$b^\alpha_\sigma = \sum_{\sigma'\beta} S^{\alpha\beta}_{\sigma\sigma'}a^\beta_{\sigma'}, \tag{4}$$

where b^α_σ and a^α_σ are the scattering operators for the outgoing and incoming states, $\sigma = \pm$ is the spin index, $\alpha = \{left, right\}$ represents the lead index, while the S matrix must be unitary, i.e., $S^\dagger S = 1$. The quantum field representing the electron state in the lead α can be expressed in terms of the scattering operators as follows:

$$\Psi_\alpha(x,t) = \sum_\sigma \int dE\rho_\alpha(E)\exp\left[-i\frac{E}{\hbar}t\right]|\sigma\rangle \times [e^{ikx}a^\alpha_\sigma(E) + e^{-ikx}b^\alpha_\sigma(E)], \tag{5}$$

where $\rho_\alpha(E) = [\sqrt{2\pi\hbar v_\alpha(E)}]^{-1}$ is the density of states of lead α, $v_\alpha(E)$ is the velocity of the electrons with wave vector $k = \sqrt{2mE}/\hbar$ and the velocity is chosen to have positive orientation for the incoming states. The spin-current density $\vec{J}^s = \Psi^\dagger\frac{\hbar}{2}\vec{\sigma}\hat{v}\Psi$ can be calculated with the approach of Ref. 15 and the result is

$$J^s_{\mu,\alpha} = \frac{1}{4\pi}\int dEdE'\ \exp\left[i\frac{(E-E')}{\hbar}t\right] \times [a^{\alpha\dagger}(E)\sigma_\mu a^\alpha(E') - b^{\alpha\dagger}(E)\sigma_\mu b^\alpha(E')], \tag{6}$$

where the following spinorial representation has been introduced

$$a^\alpha = \begin{pmatrix} a^\alpha_+ \\ a^\alpha_- \end{pmatrix} \tag{7}$$

while $a^{\alpha\dagger} = (a^{\alpha\dagger}_+, a^{\alpha\dagger}_-)$. Using the relation $\langle a^{\alpha\dagger}_\sigma(E)a^\beta_{\sigma'}(E')\rangle = \delta_{\alpha\beta}\delta_{\sigma\sigma'}\delta(E-E')f_\beta(E)$ and Eq. (4), $f_\beta(E)$ being the Fermi function of the lead β, the μth component of the spin-density current $\langle J^s_{\mu,\alpha}\rangle$ in the lead α can be written as[16]

$$\langle J^s_{\mu,\alpha}\rangle = -\frac{1}{4\pi}\sum_\beta\int dE\ \mathrm{Tr}\{S^{\alpha\beta\dagger}(E)\sigma_\mu S^{\alpha\beta}(E)\}f_\beta(E) \tag{8}$$

while using Eq. (3) the spin torque per unit of area $\mathcal{T}_\mu = \int dx\tau_\mu$ is

$$\mathcal{T}_\mu = \frac{1}{4\pi}\sum_{\alpha\beta=L,R}\int dE\ \mathrm{Tr}\{S^{\alpha\beta\dagger}(E)\sigma_\mu S^{\alpha\beta}(E)\}f_\beta(E). \tag{9}$$

When a dc voltage bias V is applied to the external leads, changing their chemical potentials in $\mu_{l,r} = E_F \pm eV/2$, the variation in the spin torque with respect to the external perturbation $w = eV/2$ can be written as $\delta_w\mathcal{T}_\mu = \partial_w\mathcal{T}_\mu\delta w$ in the linear-response regime. It is determined by the torkance $\partial_w\mathcal{T}_\mu = T_\mu$. Using Eq. (9) and taking the zero-temperature limit, we explicitly have[17]

$$T_\mu = \partial_w\mathcal{T}_\mu = \frac{1}{2\pi}\mathrm{Tr}\{\sigma_\mu(S^{21}S^{21\dagger} - S^{12}S^{12\dagger})\}|_{E=E_F}. \tag{10}$$

The torkance along the generic direction defined by the unit vector $\hat{n} = (n_x, n_y, n_z)$ is obtained as $\hat{n}\cdot\partial_w\vec{\mathcal{T}}$. Equation (10) describes the magnetic answer of the system to an external dc voltage.

IV. ALL ELECTRICAL GENERATION OF SPIN TORQUE BY QUANTUM PUMPING

In this section we discuss the generation of spin torque by means of ac external gate voltages. In particular, we generalize the notion of quantum pumping of charges due to

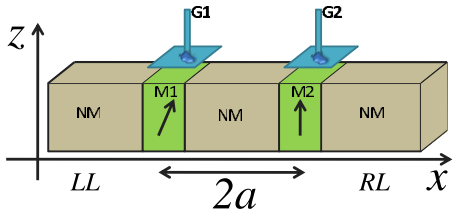

FIG. 1. (Color online) Schematic representation of the quasi-one-dimensional NM/M/NM/M/NM system described in the main text. The spin current flows along the x direction while the magnetizations M1 and M2 belong to the x-z plane.

Thouless[13] to the spin torque. In a quantum pump a dc particle current is generated by the ac adiabatic modulation of at least two out-of-phase independent parameters of the system (e.g., local magnetic fields or gate voltages) in *absence of bias*. In our calculation we will show that since pumping procedure in a magnetic layered structure can generate spin currents other than charge currents, a spin torque is generated by the gradient of spin current [see Eqs. (2) and (3)]. In particular, we focus on the system of Fig. 1 in which a microstructure made of a central nonmagnetic region (NM) is connected to two external nonmagnetic leads (*LL* and *RL*) through magnetic layers (M1 and M2) (whose width is taken less than the de Broglie wavelength). Applying the idea of pumping, we modulate in time the barriers heights at the interface between the M-NM regions by the top gates G1 and G2. In the presence of this ac modulation the scattering matrix S depends explicitly on time and the relation between incoming and outgoing states is

$$b^{\alpha}(t) = \sum_{\beta} \int dt' S^{\alpha\beta}(t,t') a^{\beta}(t'), \tag{11}$$

where the spin indices are absorbed in the spinorial notation [see Eq. (7)]. When the gates are varied adiabatically in time, an instantaneous approximation can be made, i.e., $S^{\alpha\beta}(t,t') = \delta(t-t')S^{\alpha\beta}(t)$, and thus $b^{\alpha}(t) = \Sigma_{\beta} S^{\alpha\beta}(t) a^{\beta}(t)$. Since the time dependence of the scattering matrix $S(t)$ is induced by two external parameters of the form

$$X_1(t) = X_1^0 + X_1^{\omega} \sin(\omega t),$$

$$X_2(t) = X_2^0 + X_2^{\omega} \sin(\omega t + \varphi), \tag{12}$$

then $S(t) = S(X_1(t), X_2(t))$. In particular, when the amplitude of the ac parameters is small, i.e., $X_{1,2}^{\omega} \ll X_{1,2}^0$, the scattering matrix can be expanded as follows:

$$S^{\alpha\beta}(t) \simeq S_0^{\alpha\beta} + \sum_{\eta=\pm 1} s_{\eta}^{\alpha\beta} e^{i\eta\omega t}, \tag{13}$$

where $\omega = 2\pi\nu$ is the angular frequency of the adiabatic modulation and the matrices $s_{\eta}^{\alpha\beta}$ are given by

$$s_{\eta} = -\frac{i\eta}{2} [X_1^{\omega} (\partial_{X_1} S)_0 + X_2^{\omega} e^{i\eta\varphi} (\partial_{X_2} S)_0]. \tag{14}$$

The Fourier transform of Eq. (13) is then:

$$S^{\alpha\beta}(E) = 2\pi \left[S_0^{\alpha\beta} \delta(E) + \sum_{\eta=\pm 1} s_{\eta}^{\alpha\beta} \delta(E + \eta\omega) \right]. \tag{15}$$

Consequently, the relation between the outgoing and incoming states in the Fourier space takes the following form

$$b^{\alpha}(E) = \sum_{\beta} \left[S_0^{\alpha\beta} a^{\beta}(E) + \sum_{\eta} s_{\eta}^{\alpha\beta} a^{\beta}(E + \eta\omega) \right]. \tag{16}$$

Using Eq. (16) in Eq. (6) the μ component of the spin torque per unit of area is given by

$$\mathcal{T}_{\mu} = \frac{1}{4\pi} \sum_{\eta\alpha\beta} \int dE \, \mathrm{Tr}\{ s_{\eta}^{\alpha\beta\dagger} \sigma_{\mu} s_{\eta}^{\alpha\beta} \} f_{\beta}(E + \eta\omega). \tag{17}$$

Since no bias is present between the leads $f_{\beta}(E) = f(E)$, and in the zero-temperature limit, the μth component of spin torque per unit area to leading order in the adiabatic frequency ω is

$$\mathcal{T}_{\mu} = -\frac{\hbar\omega}{4\pi} \sum_{\alpha\beta\eta} \eta \, \mathrm{Tr}\{ \sigma_{\mu} s_{\eta}^{\alpha\beta} s_{\eta}^{\alpha\beta\dagger} \}. \tag{18}$$

Above all terms independent from the external perturbation have been dropped thus the coefficient of $\hbar\omega$ in Eq. (18) is the equivalent of the torkance in the case of dc bias $T_{\mu} = \mathcal{T}_{\mu}/(\hbar\nu/2)$. Using Eq. (14) the torque can be rewritten in terms of the parametric derivatives of the scattering matrix as

$$\mathcal{T}_{\mu} = \frac{\hbar\omega X_1^{\omega} X_2^{\omega} \sin(\varphi)}{8\pi} \sum_{\alpha\beta} \mathrm{Tr}\{ A_{\mu}^{\alpha\beta} + A_{\mu}^{\alpha\beta\dagger} \}, \tag{19}$$

where we introduced the quantity $A_{\mu}^{\alpha\beta} = i(\partial_{X_2} S^{\alpha\beta\dagger})_0 \sigma_{\mu} (\partial_{X_1} S^{\alpha\beta})_0$. Equation (19) represents the torque pumped in a magnetic system and, in principle, could be very different from the one induced by a dc voltage. In the following we perform the explicit calculation for the system of Fig. 1.

V. SPIN TORQUE IN M-NM-M SYSTEMS

Here we analyze the spin torque generated in the system of Fig. 1 in the linear-response regime and in the following two situations: (i) in the presence of a dc voltage applied to the external leads; (ii) in the absence of bias and using a quantum pumping procedure. The central NM region is connected to two external leads via the thin magnetic layers M1 and M2 and without loss of generality we choose the magnetization of M2 parallel to the z axis while the magnetization of the region M1 has arbitrary direction. The distance between the two magnetic barriers is taken $2a$ and their height is controlled by the top gates G1 and G2. A minimal model for the system above is given by the following Hamiltonian

$$H = -\frac{\hbar^2}{2m} \partial_x^2 + V_m(x, \vec{\sigma}) + U(x), \tag{20}$$

where $U(x) = g_1 \delta(x+a) + g_2 \delta(x-a)$ is the barriers potential at the interface between M-NM region while $V_m(x, \vec{\sigma}) = \gamma_l \delta(x+a) \hat{n} \cdot \vec{\sigma} + \gamma_r \delta(x-a) \sigma_z$ represents the mag-

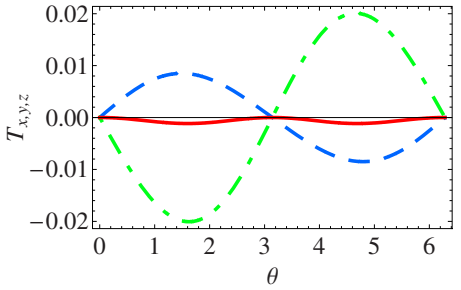

FIG. 2. (Color online) Torkance T_x (dashed line), T_y (dashed-dotted line), and T_z (full line) in units of area plotted as a function of the angle θ between M1 and M2. The parameters have been fixed as follows: $k_F a=2$, $r_1=0.5$, $r_2=1$, $\Gamma_L=0.1$, and $\Gamma_R=1$. When the magnetization directions of the layers M1 and M2 are parallel or antiparallel the torkance vanishes.

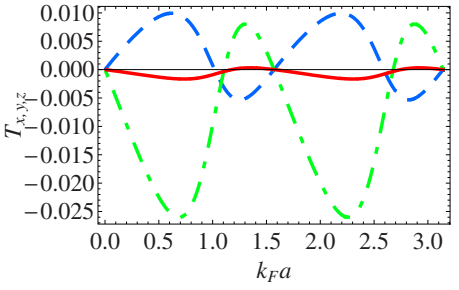

FIG. 3. (Color online) Torkance T_x (dashed line), T_y (dashed-dotted line), and T_z (full line) in units of area plotted as a function of the semidistance a between the gates G1 and G2. The parameters have been fixed as follows: $\theta=1.5$, $r_1=0.5$, $r_2=1$, $\Gamma_L=0.1$, and $\Gamma_R=1$.

netic exchange interaction between the conduction electrons spin and the magnetization of the layers M1 and M2. The scattering problem for the Hamiltonian above can be easily solved by imposing the appropriate boundary conditions on the wave functions and their derivatives at the interfaces (see, for instance, Ref. 18) and from the knowledge of the scattering matrix the spin torque $\mathcal{T}_\mu$ can be calculated using the equations of the previous sections. The following consideration is in order here: the presence of two magnetic layers has the effect of allowing for multiple scattering of the electrons between them, which gives rise to an explicit asymmetry of the spin current and produces a finite spin-torque effect. In the following we employ the dimensionless quantities: $r_1=\frac{2mg1}{\hbar^2 k_F}$, $r_2=\frac{2mg2}{\hbar^2 k_F}$, $\Gamma_R=\frac{2m\gamma_r}{\hbar^2 k_F}$, and $\Gamma_L=\frac{2m\gamma_l}{\hbar^2 k_F}$, where k_F is the Fermi wavelength, $m=\alpha m_e$ is the effective electron mass, while α represents the ratio between the effective and the bare electron mass m_e. The distances are made dimensionless by multiplying by k_F, i.e., $a\to k_F a$.

A. Linear response of the spin torque by means of dc voltage bias

Here we present the results of the spin torque per unit of area under small variation of dc voltage bias $eV/2$, i.e., the torkance. The explicit expression of the spin torque in terms of the electron-spin density, the exchange couplings and the noncollinearity between the magnetizations of magnetic layers M1 and M2 is reported in Appendix. In the following we use polar coordinates for the magnetizations $\vec{M}_1=M_1\hat{n}_1$, $\hat{n}_1=[\sin(\theta)\cos(\phi),\sin(\theta)\sin(\phi),\cos(\theta)]$, and assume that $\vec{M}_1$ and $\vec{M}_2$ lie in the plane x-z. In this case we have $\hat{n}_1=[\sin(\theta),0,\cos(\theta)]$, where the θ represents the angle between $\vec{M}_1$ and $\vec{M}_2$ [notice that $\hat{n}_2=(0,0,1)$].

In Fig. 2 the three components of the torkance are shown as a function of angle θ between the magnetizations of the regions M1 and M2 and by fixing the remaining parameters as follows: $k_F a=2$, $r_1=0.5$, $r_2=1$, $\Gamma_L=0.1$, and $\Gamma_R=1$. Similarly to other works, we find that all the torque components and consequently the torkance vanish when M1 and M2 are parallel or antiparallel, as explicitly shown in Appendix. Furthermore, the z component T_z of the torkance is very small compared to T_x and T_y while the component T_y is the strongest. This last component of the torkance follows a sin θ behavior for the specific values of magnetic interactions considered in Fig. 2 ($\Gamma_R \gg \Gamma_L$).[19] This can be easily understood as follows: when the nonspin-polarized electrons are incident on the magnetic layer M2, spin-filtering effects removes the component of the spin angular momentum perpendicular to the layer magnetization from the current acting as a polarizer along the z direction. Thus the polarized electrons with spin density S_z scattered off M2 and incident on M1 generate an effective torque on the layer momentum M1 proportional to the sin θ [see Eq. (A2)]. The negative sign of T_y is due to the fact that electrons with spins parallel to the moment of the magnetic region M2 have a larger transmission probability compared to those antiparallel. In the case of symmetric exchange couplings $\Gamma_R \sim \Gamma_L$ we find that only the component of the torkance orthogonal to the plane of the magnetizations T_y acquires relevant values while T_x, T_z are suppressed and the dependence on the angle θ deviates from the simple sin θ.

In Fig. 3 the components of the torkance are shown as a function of the semidistance a between the gates G1 and G2 and by fixing the remaining parameters as follows: $\theta=1.5$, $r_1=0.5$, $r_2=1$, $\Gamma_L=0.1$, and $\Gamma_R=1$. For a mesoscopic system characterized by a de Broglie wavelength $\lambda \approx 20-30$ nm the dimensionless distance $k_F a=1$ would correspond to 3.18–4.78 nm. As shown in the figure, the torkance presents a characteristic oscillatory behavior with the semilength of the central region a. These oscillations can be regarded as a quantum-size effect. They reflect the perfect ballistic regime of electron transport through the spin valve. The physical mechanism behind the oscillations is the interference effect of the electrons propagating across the nonmagnetic-magnetic interface from the right lead to the left lead and electrons propagating backward.[20] The particular value of the oscillation follows from the values of the spin-dependent Fermi wave vector.

In Fig. 4 we plot $T_{x,y,z}$ as a function of the strength r_2 of the right barrier (controllable via the gate G2) by fixing the other parameters as: $\theta=1.5$, $r_1=0.5$, $k_F a=2$, $\Gamma_L=0.1$, and $\Gamma_R=1$. The torkance of course depends crucially on the transparency of the barrier and thus the components $T_{x,y}$ decreases with increasing barrier height becoming comparable to T_z. An interesting feature appears by increasing the Zeeman in-

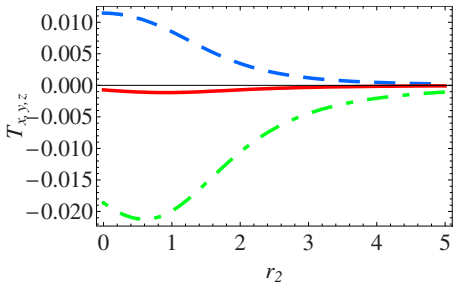

FIG. 4. (Color online) Torkance T_x (dashed line), T_y (dashed-dotted line), and T_z (full line) in units of area plotted as a function of the nondimensional barrier strength r_2 controlled by G2. The parameters have been fixed as follows: $\theta=1.5$, $r_1=0.5$, $k_F a=2$, $\Gamma_L=0.1$, and $\Gamma_R=1$.

teraction Γ_L as shown in Fig. 5: for values of Γ_L above 0.2 the z component of the torkance T_z starts to assume relevant values. In fact the magnetic interaction becomes more effective in aligning the electron spins along the magnetic moment of the layer M1 thus reducing the contribution to the gradient of spin current.

B. Spin-torque generation by means of adiabatic quantum pumping

An alternative way to generate a spin torque is the adiabatic quantum pumping technique. As explained above we keep the two external leads at the same chemical potential and in order to generate a spin current we modulate out-of-phase in time the two barrier heights r_1 and r_2 by the gate voltages G1 and G2,

$$r_1(t) = r_1^0 + r_1^\omega \sin(\omega t),$$

$$r_2(t) = r_2^0 + r_2^\omega \sin(\omega t + \varphi). \tag{21}$$

Thus by using Eq. (19) the μth component of the torque in the adiabatic regime, i.e., to leading order in the frequency pump, is given by

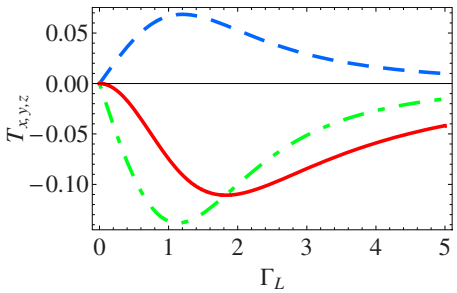

FIG. 5. (Color online) Torkance T_x (dashed line), T_y (dashed-dotted line), and T_z (full line) plotted in units of area as a function of Γ_L controlled by the magnetic momentum in the region M1. The remaining parameters have been fixed as follows: $\theta=1.5$, $r_1=0.5$, $r_2=0.8$, $k_F a=2$, and $\Gamma_R=1$.

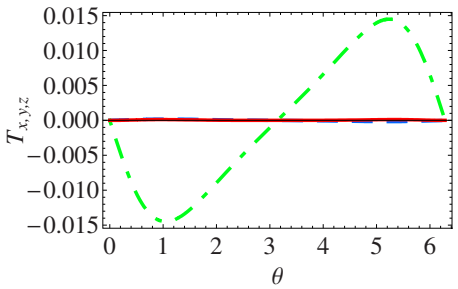

FIG. 6. (Color online) Torkance T_x (dashed line), T_y (dashed-dotted line), and T_z (full line) in units of area plotted as a function of θ between M1 and M2. The remaining parameters have been fixed as follows: $r_1^\omega=r_2^\omega=0.2$, $\Gamma_L=0.9$, $r_1^0=0.5$, $r_2^0=0.3$, $k_F a=1$, and $\Gamma_R=1$.

$$\mathcal{T}_\mu = \frac{\hbar\omega r_1^\omega r_2^\omega \sin(\varphi)}{8\pi} \sum_{\alpha\beta} \mathrm{Tr}\{A_\mu^{\alpha\beta} + A_\mu^{\alpha\beta\dagger}\}. \tag{22}$$

In the weak pumping regime (i.e., $r_i^0 \gg r_i^\omega$) considered here, $\mathcal{T}_\mu$ presents a $\sin(\varphi)$ behavior with respect to the pumping phase φ and thus in the following analysis we set $\varphi=\pi/2$.

Concerning the frequencies of the pump, we can safely consider as adiabatic the frequencies for which $\hbar\omega$ is smaller than the first gap in the electron energy spectrum such that the system lies in its ground state.[13] For simplicity, by considering the energy spectrum of a particle confined in a box, we easily find that the threshold frequency is $\tilde{\nu} \sim \frac{h}{2m^\star L^2}$, where L is the length of the system while $m^\star=\alpha m_e$ is the effective mass of the electrons. Thus for a system with $L=1.5$ μm and effective mass ratio $\alpha=0.023$, $\tilde{\nu}\approx 43.4$ GHz which is consistent with the values of the frequencies of quantum pumping in quantum dots. For a smaller system characterized by $L=0.5$ μm and $\alpha=0.023$ we obtain $\tilde{\nu} \approx 396.5$ GHz which is a more convenient value to achieve in experiments. In Fig. 6 we plot the components T_μ as a function of the angle θ between the magnetization M1 and M2 and by fixing the other parameters as follows: $r_1^\omega=r_2^\omega=0.2$, $\Gamma_L=0.9$, $r_1^0=0.5$, $r_2^0=0.3$, $k_F a=1$, and $\Gamma_R=1$. Compared to the case of dc bias, the θ dependence of the torkance is not a simple $\sin\theta$ form because the strength of the magnetic interactions Γ_L and Γ_R is comparable and thus both $\cos\theta$ and $\sin\theta$ terms contribute (see Appendix). Moreover as in the previous analysis, while the components of the torkance T_x and T_z assume very small values in the parameter region considered, the T_y component presents relevant values. In Fig. 7 we show the spin torkance $T_{x,y,z}$ as a function of the semidistance a between the gates G1 and G2, for the remaining parameters: $r_1^\omega=r_2^\omega=0.2$, $\Gamma_L=0.9$, $r_1^0=0.5$, $r_2^0=0.3$, $\Gamma_R=1$, and $\theta=1$. Compared to the case in which the spin torque is generated by an external dc bias, more harmonics are present in the torque dependence on a. This behavior can be qualitatively explained by the fact that the torque generated by the pumping procedure is related to the parametric derivatives of the scattering matrix. In Fig. 8 we show the spin torkance components $T_{x,y,z}$ as a function of the static part of the dimensionless barrier strength r_2^0 controlled by G2 while the remaining parameters have been fixed as follows: $r_1^\omega=r_2^\omega$

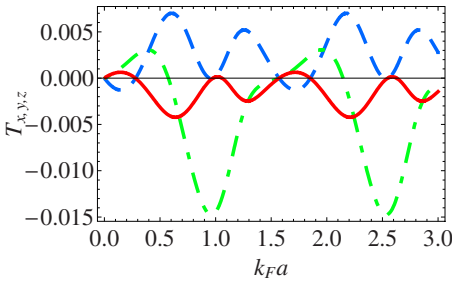

FIG. 7. (Color online) Torkance T_x (dashed line), T_y (dashed-dotted line), and T_z (full line) in units of area plotted as a function of the semidistance a between the gates G1 and G2. The remaining parameters have been fixed as follows: $r_1^\omega = r_2^\omega = 0.2$, $\Gamma_L = 0.9$, $r_1^0 = 0.5$, $r_2^0 = 0.3$, $\Gamma_R = 1$, and $\theta = 1$.

$=0.2$, $\Gamma_L=0.9$, $r_1^0=0.5$, $k_F a=1$, $\Gamma_R=1$, and $\theta=1$. As shown, for increasing values of the static barrier strength r_2^0 the torque pumped in the system vanishes. Indeed, the reduction in the spin current from the external leads reduces the gradient of the current and thus the spin torque is strongly suppressed. In the case of pumping, the suppression of the torque by increasing the barriers height may be in general stronger compared to the dc case. In Fig. 9 we show the spin torkance components $T_{x,y,z}$ as a function of the Zeeman interaction Γ_L for the other parameters: $r_1^\omega = r_2^\omega = 0.2$, $r_2^0 = 1$, $r_1^0 = 0.5$, $k_F a = 1$, $\Gamma_R = 1$, and $\theta = 1$. A behavior similar to the one presented in Fig. 5 is found. The magnetic interaction of the electron spins with the magnetic moment of M1 causes a suppression of the torque above $\Gamma_L \approx 1.7$ thus acting like an energy barrier for the electrons.

VI. LOCAL SPIN TORQUE AND SPIN VALVES CASE

Up to now the properties of the total spin torque (i.e., the sum of the spin torques generated on the two magnetic layers) under the effect of dc or ac external forcing terms have been studied. However, when the magnetization direction of a given layer is fixed (fixed layer) only the magnetization direction of the other, the so-called free layer, can be affected by the local torque induced by the gradient of a spin-polarized current. In this situation, typical of spin-valve experimental setups, the torque generated on the free layer has

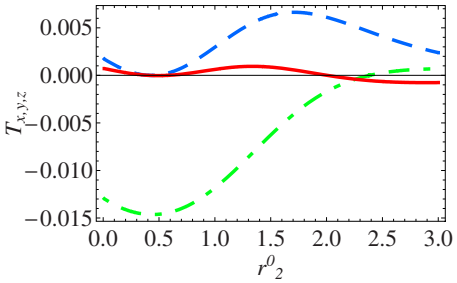

FIG. 8. (Color online) Torkance T_x (dashed line), T_y (dashed-dotted line), and T_z (full line) in units of area plotted as a function of the static part of the dimensionless barrier strength r_2^0. The remaining parameters have been fixed as follows: $r_1^\omega = r_2^\omega = 0.2$, $\Gamma_L = 0.9$, $r_1^0 = 0.5$, $k_F a = 1$, $\Gamma_R = 1$, and $\theta = 1$.

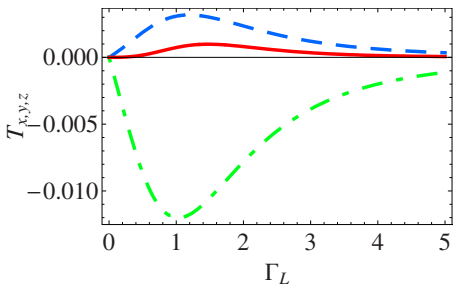

FIG. 9. (Color online) Torkance T_x (dashed line), T_y (dashed-dotted line), and T_z (full line) in units of area plotted as a function of Γ_L. The remaining parameters have been fixed as follows: $r_1^\omega = r_2^\omega = 0.2$, $r_2^0 = 1$, $r_1^0 = 0.5$, $k_F a = 1$, $\Gamma_R = 1$, and $\theta = 1$.

important implications due to the possibility of producing a current-induced magnetization reversal detectable, for instance, by magnetoresistance measurements. In our setup of Fig. 1, suppose the layer M1 represents the free layer, being M2 the fixed layer whose magnetization direction is $\hat{n}_2 = (0,0,1)$. The torque generated on M1, i.e., $\vec{\mathcal{T}}_1$, lies on the plane perpendicular to the magnetization direction $\hat{n}_1 = [\sin(\theta), 0, \cos(\theta)]$ of the free layer since $\hat{n}_1 \cdot \vec{\mathcal{T}}_1 = 0$ [see the structure of Eq. (A1) in Appendix]. For the configuration in Fig. 1, it is possible to write the projection of $\vec{\mathcal{T}}_1$ parallel and perpendicular to the mentioned plane by introducing the following set of basis vectors

$$\hat{\nu}_\perp = \frac{\hat{n}_2 \times \hat{n}_1}{|\hat{n}_2 \times \hat{n}_1|} = \hat{y},$$

$$\hat{\nu}_\parallel = \frac{\hat{n}_1 \times (\hat{n}_2 \times \hat{n}_1)}{|\hat{n}_1 \times (\hat{n}_2 \times \hat{n}_1)|} = -\hat{x}\cos(\theta) + \hat{z}\sin(\theta). \quad (23)$$

The torque acting on the free layer can thus be presented in the form $\vec{\mathcal{T}}_1 = \mathcal{T}_1^\parallel \hat{\nu}_\parallel + \mathcal{T}_1^\perp \hat{\nu}_\perp$, where

$$\mathcal{T}_1^\parallel = \vec{\mathcal{T}}_1 \cdot \hat{\nu}_\parallel = \mathcal{T}_{1,y},$$

$$\mathcal{T}_1^\perp = \vec{\mathcal{T}}_1 \cdot \hat{\nu}_\perp = -\mathcal{T}_{1,x}\cos(\theta) + \mathcal{T}_{1,z}\sin(\theta). \quad (24)$$

To calculate the torque components acting on the free layer at $x=-a$ we make use of the scattering matrix approach presented in Sec. III and of the following formula

$$\langle \mathcal{T}_\mu(x=-a)\rangle = \frac{2\gamma_l}{\hbar}[\hat{n}(x=-a) \times \langle \vec{S}(x=-a)\rangle]_\mu, \quad (25)$$

where $\hat{n}(x=-a) \equiv \hat{n}_1$ and the average spin density $\langle \vec{S}(x=-a)\rangle$ is calculated using its definition and Eq. (5). The explicit expressions in the dc case are shown below

$$\mathcal{T}_1^\parallel = -\frac{w\Gamma_L}{2\pi}\mathrm{Tr}[\sigma_y S^{12} S^{12\dagger}],$$

$$\mathcal{T}_1^\perp = \frac{w\Gamma_L}{2\pi}\mathrm{Tr}\{[\sin(\theta)\sigma_z - \cos(\theta)\sigma_x] S^{12} S^{12\dagger}\}, \quad (26)$$

where $w = eV/2$. The torque components acting on the free layer in the case of pumping are instead

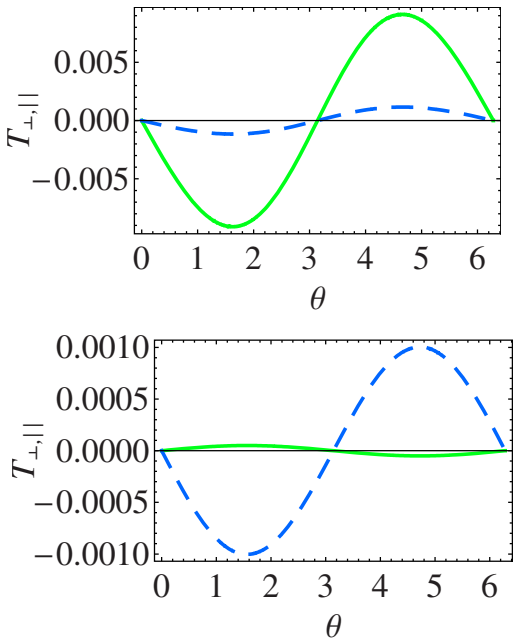

FIG. 10. (Color online) Torkance $T_\perp$ (full line), $T_\parallel$ (dashed line) in units of area plotted as a function of the angle θ between M1 and M2. The remaining parameters have been fixed for the upper panel as: $k_F a=2$, $r_1=0.5$, $r_2=1$, $\Gamma_L=0.1$, and $\Gamma_R=1$ while for the lower panel: $k_F a=2$, $r_1=0$, $r_2=0$, $\Gamma_L=0.1$, and $\Gamma_R=1$. Notice that the phenomenology observed in the spin-valve systems, i.e., $T_\parallel \gg T_\perp$ is visible in the lower panel.

$$\mathcal{T}_1^{\parallel} = \frac{\hbar\omega\Gamma_L}{8\pi} r_1^\omega r_2^\omega \sin(\varphi) \sum_\beta \mathrm{Tr}[A_y^{1\beta} + A_y^{1\beta\dagger}],$$

$$\mathcal{T}_1^{\perp} = -\frac{\hbar\omega\Gamma_L}{8\pi} r_1^\omega r_2^\omega \sin(\varphi) \sum_\beta \mathrm{Tr}[\sin(\theta)(A_z^{1\beta} + A_z^{1\beta\dagger}) - \cos(\theta) \times (A_x^{1\beta} + A_x^{1\beta\dagger})], \quad (27)$$

where $A_\mu^{\alpha\beta} = i(\partial_{r_2} S^{\alpha\beta})_0^\dagger \sigma_\mu (\partial_{r_1} S^{\alpha\beta})_0$ with $\mu = x, y, z$. Equations (26) and (27) represents the main result of this work concerning the spin valves context.

A. Results for the dc case

In Sec. VI A we present numerical results for the perpendicular and parallel components of the spin torque acting on the free layer as obtained by Eq. (26). In the figures the torque components will be normalized to the quantity $w = eV/2$ and thus we define $T_\parallel = \mathcal{T}_1^{\parallel}/w$ and $T_\perp = \mathcal{T}_1^{\perp}/w$.

In the upper panel of Fig. 10, we report the torkance $T_\perp$ (full line) and $T_\parallel$ (dashed line) as a function of the angle θ between the M1 and M2 and by setting the remaining parameters as: $k_F a=2$, $r_1=0.5$, $r_2=1$, $\Gamma_L=0.1$, and $\Gamma_R=1$. As shown, the perpendicular component of the torkance $T_\perp$ takes values greater than the parallel component while a sinusoidal behavior with respect to θ is observed for both curves. Putting to zero the electrostatic gates r_1 and r_2 (lower panel) a strong suppression of the perpendicular component of the torkance is observed while the parallel component $T_\parallel$ remains almost unchanged. The strong perpendicular component of the torkance can thus be related to the presence of local electrostatic potentials along the transport direction. This behavior can also be understood when looking at torkance as a function of the magnetization strength Γ_L of the free layer. In the upper panel of Fig. 11 we report the behavior of $T_{\perp,\parallel}$ as a function of Γ_L by setting the remaining parameters as: $k_F a=2$, $r_1=0$, $r_2=0$, $\theta=\pi/2$, and $\Gamma_R=1$. In that figure computed in the absence of local electrostatic potentials $r_{1,2}$, when Γ_L takes values lesser than $\Gamma_L \sim 0.2$, one observes that the condition $T_\parallel \gg T_\perp$ is verified. On the other hand, when some electrostatic potential is present, as shown in the lower panel of Fig. 11, the parallel and perpendicular component of the torkance take similar values for $0 < \Gamma_L < 0.15$. These properties are important in understanding the relevant parameters region where the proposed model is able to capture the spin-valve phenomenology. In fact in such systems, a well-known property is that the parallel component of the torque is dominant over the perpendicular one. In the upper panel of Fig. 12 we represent the components of the torkance as a function of the semidistance $k_F a$ between the electrostatic gates G1 and G2 by setting the remaining parameters as: $r_1=0.5$, $r_2=1$, $\theta=1.5$, $\Gamma_L=0.1$, and $\Gamma_R=1$. When the strength of the electrostatic local potential $r_{1,2}$ is set to zero, as done in the lower panel of the same figure, $T_\perp$ becomes negligible and the $T_\parallel$ component shows an oscillating behavior with respect to $k_F a$ as already shown in Fig. 3. In particular, for small values of r_2 and by setting, for in-

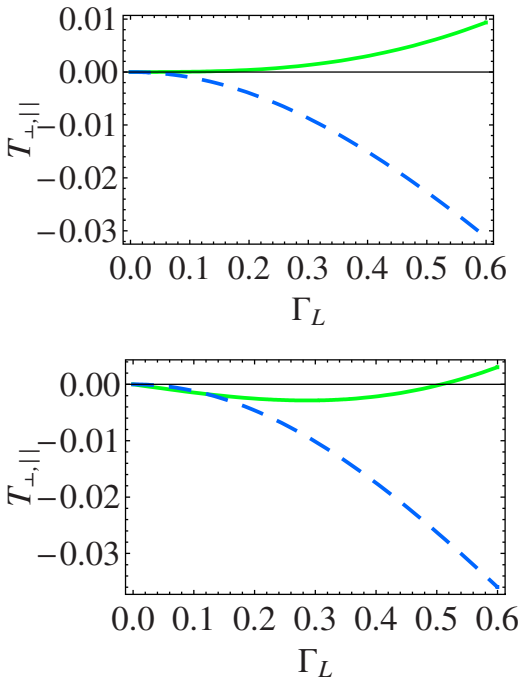

FIG. 11. (Color online) Torkance $T_\perp$ (full line), $T_\parallel$ (dashed line) in units of area plotted as a function of Γ_L. The remaining parameters have been fixed for the upper panel as: $k_F a=2$, $r_1=0$, $r_2=0$, $\theta=\pi/2$, and $\Gamma_R=1$ while for the lower panel: $k_F a=2$, $r_1=0$, $r_2=0.15$, $\theta=\pi/2$, and $\Gamma_R=1$. Notice that the increasing of the barrier strength r_2 (lower panel) produces an enhancement of the perpendicular component of the spin torque as evident in the region $0 < \Gamma_L < 0.15$.

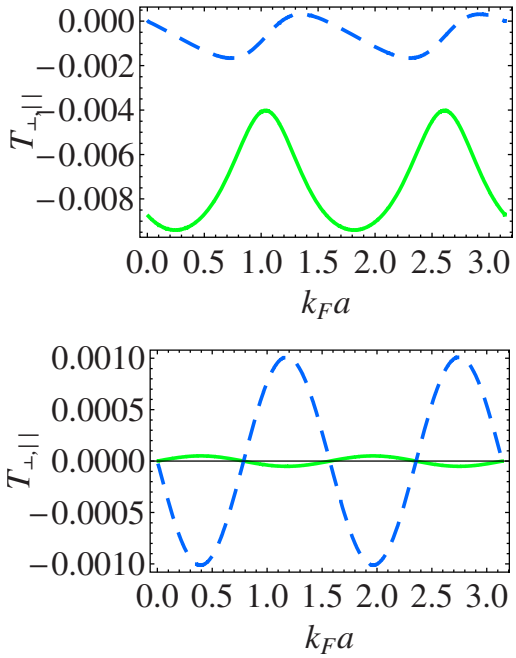

FIG. 12. (Color online) Torkance $T_\perp$ (full line), $T_\parallel$ (dashed line) in units of area plotted as a function of the semidistance $k_F a$ between the gates G1 and G2. The remaining parameters have been fixed for the upper panel as: $r_1=0.5$, $r_2=1$, $\theta=1.5$, $\Gamma_L=0.1$, and $\Gamma_R=1$. The lower panel has been computed setting the $r_1=r_2=0$, being the remaining parameters unchanged with respect to the upper panel. Notice that the perpendicular component of the spin torque is strongly enhanced by the presence of local electrostatic potentials (i.e., nonvanishing values of $r_{1,2}$).

stance, the model parameters as $r_1=0$, $k_F a=2$, $\theta=\pi/2$, $\Gamma_L=0.15$, and $\Gamma_R=1$, we observe that the torkance behavior can be well represented by the relations $T_\perp(r_2)\simeq-\alpha r_2$, $T_\parallel(r_2)\simeq-\beta$, where $\alpha\simeq 1.43\times10^{-2}$ and $\beta\simeq 2.25\times10^{-3}$. This behavior is qualitatively correct for $0<r_2<0.1$ and clarifies the role of the scattering potential in originating the perpendicular component of the spin torque even in the linear response to the dc bias applied to the nanostructure.[21]

B. Results for the pumping case

In Sec. VI B we present numerical results for the perpendicular and parallel components of the spin torque generated

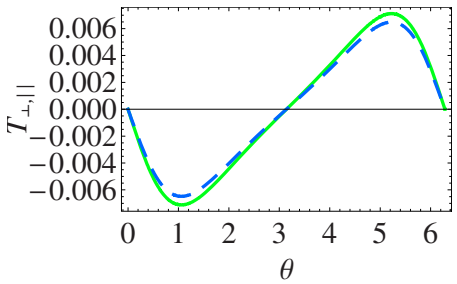

FIG. 13. (Color online) Torkance $T_\perp$ (full line), $T_\parallel$ (dashed line) in units of area plotted as a function of θ between M1 and M2. The remaining parameters have been fixed as follows: $r_1^\omega=r_2^\omega=0.2$, $\Gamma_L=0.9$, $r_1^0=0.5$, $r_2^0=0.3$, $k_F a=1$, and $\Gamma_R=1$.

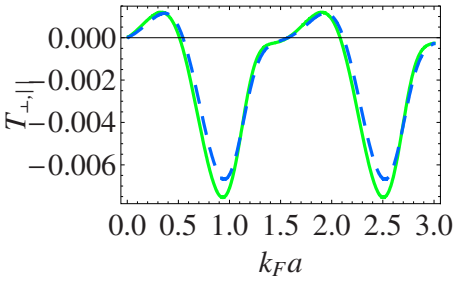

FIG. 14. (Color online) Torkance $T_\perp$ (full line), $T_\parallel$ (dashed line) in units of area plotted as a function of the semidistance a between the gates G1 and G2. The remaining parameters have been fixed as follows: $r_1^\omega=r_2^\omega=0.2$, $\Gamma_L=0.9$, $r_1^0=0.5$, $r_2^0=0.3$, $\Gamma_R=1$, and $\theta=1$.

on the free layer by using Eq. (27) in the case of ac external potentials. In the figures the torque components are normalized with respect to the quantity $\hbar\nu/2$ and thus we set $T_\parallel=T_1^\parallel/(\hbar\nu/2)$ and $T_\perp=T_1^\perp/(\hbar\nu/2)$ while the pumping phase will be set to $\varphi=\pi/2$ as done in previous sections. In Fig. 13 $T_\perp$ (full line) and $T_\parallel$ (dashed line) are shown as a function of the angle θ. Due to the finite values of the electrostatic potentials $r_{1,2}$ we observe that $T_\perp\sim T_\parallel$. In particular, the parameters of this figure have been chosen as in Fig. 6 where the total torkance has been represented. Apart from some similarities between the behavior of T_y in Fig. 6 and $T_\perp$ in Fig. 13 [notice that $T_\perp(\theta=1)\sim T_y(\theta=1)/2$] a direct comparison between the total torque discussed in the previous sections and the torque acting on the free layer is not possible since a local coordinates system has been used instead of the global one employed in the first part of this paper. In Fig. 14 we report the torkance components as a function of the semidistance $k_F a$ between M1 and M2 setting the remaining parameters as done in Fig. 7. Indeed, one can notice that the torque components present similar strength and oscillatory behavior of the one displayed by T_y in Fig. 7. To complete our analysis, we compute the torkance $T_{\perp,\parallel}$ as a function of the static part of the dimensionless barrier strength r_2^0 by setting the model parameters as done in Fig. 8. As shown in Fig. 15 for large values of the static part of the local potential r_2^0 the torque components become negligible as already discussed in previous sections. Very interestingly, for values of r_2^0 close to 1.4 the proposed device can selectively pump on the free-layer nonvanishing values of $T_\perp$ or $T_\parallel$.

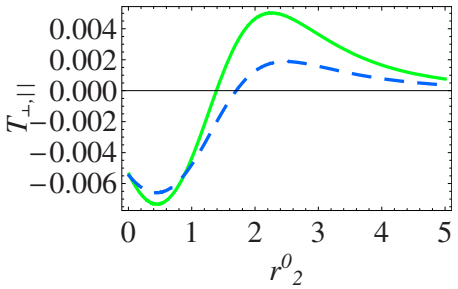

FIG. 15. T(Color online) orkance $T_\perp$ (full line), $T_\parallel$ (dashed line) in units of area plotted as a function of the static part of the dimensionless barrier strength r_2^0. The remaining parameters have been fixed as follows: $r_1^\omega=r_2^\omega=0.2$, $\Gamma_L=0.9$, $r_1^0=0.5$, $k_F a=1$, $\Gamma_R=1$, and $\theta=1$.

VII. CONCLUSIONS

Within the scattering matrix approach we studied the spin torque and its linear response generated by dc or ac external perturbations acting on a quasi-one-dimensional multilayered system consisting of a sequence of magnetic/nonmagnetic regions. In particular, we studied the spin torque of a magnetic-nonmagnetic-magnetic trilayer connected to metallic nonmagnetic leads. We have focused on the effect of spin filtering as the mechanism for current-induced torque, i.e., the difference in the transmission and reflection probabilities for electrons with spins parallel and antiparallel to the moments of the magnetic layers. The torkance generated by the application of a dc bias to the external leads was analyzed as a function of the relative orientation θ between the magnetizations of the magnetic regions, the length $2a$ of the nonmagnetic spacer, the barriers transparencies and the Zeeman couplings. From the analysis we observed that the spin torque and the torkance vanish when the magnetizations of M1 and M2 are parallel or antiparallel, while an oscillating behavior was observed as a function of a, indicating a quantum-size effect. When the transparencies of the tunnel barriers at the interfaces between the magnetic/nonmagnetic layers are lowered, a strong suppression of the torkance is observed due to the reduction of the spin fluxes through the barriers. Similar effects were found as a function of the strength of the magnetic interaction Γ_L. As an alternative to considering external dc bias, we proposed a current-induced spin torque based on quantum pumping, generalizing the original idea of Thouless for the charges.[13] We formulated a scattering matrix theory of the spin-torque pumping. By modulating in time the strength of the two out-of-phase tunnel barriers at the interface between the magnetic/nonmagnetic layers, spin-polarized currents were produced in the leads and a gradient of spin current responsible for the spin torque was generated. By studying the spin-torque components to leading order in the pumping frequency, we observed different signatures of the magnetic reversal mechanism due to the pumping procedure. For instance, within the weak pumping limit additional harmonics were observed in the oscillations of T_μ vs the length of the nonmagnetic region $2a$ and a stronger suppression of the spin torque at increasing the barrier heights. Thus the pumping mechanism could offer an additional tool to study experimentally the magnetic response of metallic heterostructures. We have limited our analysis to the quasi-one-dimensional layered structure but we expect sizable changes in the two-dimensional case. In fact when integrating over all the Fermi surface there is a reduction in the transverse spin components because of phase cancellation effects in the distribution of the spin-rotation angles and an investigation along this direction is in progress. Experimentally, current-induced spin torque has been realized in Co/Cu/Co sandwich structures[22,23] and in Py/Cu/Py heterostructures.[24] Our proposal can also be realized by using two ferromagnetic EuS barriers coupled to Al leads and separated by an Al_2O_3 spacer of few tens of nanometers by modifying, for instance, the experimental setup studied in Ref. 25.

APPENDIX: ANALYTICAL EXPRESSION OF THE TOTAL SPIN TORQUE GENERATED ON THE M-NM-M SYSTEM

We report the explicit expression of the total spin torque ($\mathcal{T}_\mu = \mathcal{T}_{\mu,l} + \mathcal{T}_{\mu,r}$) in terms of the exchange interactions, spin densities, and noncollinearity between the magnetizations. Starting from Eqs. (2) and (3) and considering the case in which the exchange interaction between the incident spins and the magnetizations of M1 and M2 is of the form $\gamma(x) = \gamma_l \delta(x+a) + \gamma_r \delta(x-a)$, we get the following expression for the μth component of the torque

$$\mathcal{T}_\mu = \frac{2}{\hbar}\{\gamma_l[\hat{n}(x=-a) \times \vec{S}(x=-a)]_\mu + \gamma_r[\hat{n}(x=a) \times \vec{S}(x=a)]_\mu\}, \tag{A1}$$

where $\hat{n}(x=-a) = [\sin(\theta), 0, \cos(\theta)]$, $\hat{n}(x=a) = (0,0,1)$, while $\vec{S}(x=\pm a) = \Psi^\dagger(\pm a)\frac{\hbar}{2}\vec{\sigma}\Psi(\pm a)$ is the spin density at $x=\pm a$. After explicit manipulation of Eq. (A1), one obtains the expression of the total torque

$$\vec{\mathcal{T}} = \frac{2}{\hbar}\{-\hat{x}[\gamma_r S_y(a) + \gamma_l S_y(-a)] + \hat{y}[\gamma_l \cos(\theta) S_x(-a) + \gamma_r S_x(a) - \gamma_l \sin(\theta) S_z(-a)] + \hat{z}[\gamma_l S_y(-a)\sin(\theta)]\}, \tag{A2}$$

consisting of the sum of the spin torque delivered on the left and right magnetic layer. Equation (A2) shows that for $\theta = 0, \pi$ the spin torque $\vec{\mathcal{T}}$ is identically zero. Indeed, for collinear magnetizations located at $x=\pm a$, the only nonvanishing component of the spin density is S_z (while $S_x = S_y = 0$) but it does not contribute to the torque since its prefactor is $\sin(\theta)$.

Finally, the total torque, as described in this appendix, can be a meaningful quantity in characterizing the domain-wall motion induced in magnetic nanowires (in the latter case the system depicted in Fig. 1 is imagined as a single magnetic domain[26]), while in the spin valves case Eqs. (26) and (27) should be used.

[1] For a review: collection of articles in S. S. P. Parkin, IBM J. Res. Dev. **42**, 3 (1998).

[2] L. Berger, Phys. Rev. B **54**, 9353 (1996).

[3] J. Slonczewski, J. Magn. Magn. Mater. **159**, L1 (1996).

[4] P. M. Krstajić, M. Keller, and F. M. Peeters, Phys. Rev. B **77**, 174428 (2008).

[5] A. Brataas, Y. V. Nazarov, and G. E. W. Bauer, Phys. Rev. Lett. **84**, 2481 (2000).

[6] X. Waintal, E. B. Myers, P. W. Brouwer, and D. C. Ralph, Phys. Rev. B **62**, 12317 (2000).

[7] K. Carva and I. Turek, Phys. Rev. B **76**, 104409 (2007).

[8] C. Heiliger and M. D. Stiles, Phys. Rev. Lett. **100**, 186805 (2008).

[9] M. D. Stiles and A. Zangwill, J. Appl. Phys. **91**, 6812 (2002).

[10] J. Xiao, G. E. W. Bauer, and A. Brataas, Phys. Rev. B **77**, 224419 (2008).
[11] S. Wang, Y. Xu, and K. Xia, Phys. Rev. B **77**, 184430 (2008).
[12] M. D. Stiles and A. Zangwill, Phys. Rev. B **66**, 014407 (2002); P. M. Haney, D. Waldron, R. A. Duine, A. S. Nunez, H. Guo, and A. H. MacDonald, *ibid.* **76**, 024404 (2007); C. Heiliger, M. Czerner, B. Yu. Yavorsky, I. Mertig, and M. D. Stiles, J. Appl. Phys. **103**, 07A709 (2008).
[13] D. J. Thouless, Phys. Rev. B **27**, 6083 (1983).
[14] Notice that when the vector potential along the transport direction A_x is included in the theory, the spin-current density takes the form $J^s_\mu(A_x)=J^s_\mu(A_x=0)-\frac{eA_x}{m}S_\mu$, Eq. (2) being unchanged.
[15] M. Büttiker, Phys. Rev. B **46**, 12485 (1992).
[16] P. Sharma and P. W. Brouwer, Phys. Rev. Lett. **91**, 166801 (2003); P. Sharma and P. W. Brouwer, arXiv:cond-mat/0306001v2.
[17] K. Carva and I. Turek, Phys. Rev. B **80**, 104432 (2009).
[18] Y. Chen, X. Zhao, and Y.-Q. Li, Semicond. Sci. Technol. **19**, 930 (2004).
[19] The asymmetry in the magnitudes of the exchange couplings can be achieved either by applying an external local field that can induce a giant Zeeman splitting between M1 or M2 and the NM central region or by considering different ferromagnets one of which could be a ferromagnetic semiconductor [e.g., (II,Mn)VI material] which has a huge gyromagnetic factor.
[20] I. Theodonis, A. Kalitsov, and N. Kioussis, Phys. Rev. B **76**, 224406 (2007).
[21] For a recent work concerning nontrivial effects induced by the bias in spin valves see: P. M. Haney, C. Heiliger, and M. D. Stiles, Phys. Rev. B **79**, 054405 (2009); see also A. Kalitsov, M. Chshiev, I. Theodonis, N. Kioussis, and W. H. Butler, *ibid.* **79**, 174416 (2009); I. Theodonis, N. Kioussis, A. Kalitsov, M. Chshiev, and W. H. Butler, Phys. Rev. Lett. **97**, 237205 (2006).
[22] J. A. Katine, F. J. Albert, R. A. Buhrman, E. B. Myers, and D. C. Ralph, Phys. Rev. Lett. **84**, 3149 (2000).
[23] E. B. Myers, D. C. Ralph, J. A. Katine, R. N. Louie, and R. A. Buhrman, Science **285**, 867 (1999).
[24] M. AlHajDarwish, H. Kurt, S. Urazhdin, A. Fert, R. Loloee, W. P. Pratt, Jr., and J. Bass, Phys. Rev. Lett. **93**, 157203 (2004).
[25] G.-X. Miao, M. Müller, and J. S. Moodera, Phys. Rev. Lett. **102**, 076601 (2009).
[26] For a simple model of domain wall in magnetic nanowires see: V. K. Dugaev, V. R. Vieira, P. D. Sacramento, J. Barnaś, M. A. N. Araújo, and J. Berakdar, Int. J. Mod. Phys. B **21**, 1659 (2007).